








Steady-state entanglement generation for nondegenerate qubits

Murilo H. Oliveira ^{1,*}, Gerard Higgins ^{2,†}, Chi Zhang ^{2,‡}, Ana Predojević ², Markus Hennrich ²,
Romain Bachelard ^{1,3} and Celso J. Villas-Boas ¹

¹*Departamento de Física, Universidade Federal de São Carlos, P.O. Box 676, 13565-905 São Carlos, São Paulo, Brazil*

²*Department of Physics, Stockholm University, 10691 Stockholm, Sweden*

³*Université Côte d'Azur, CNRS, Institut de Physique de Nice, 06560 Valbonne, France*



(Received 21 May 2022; revised 23 November 2022; accepted 17 January 2023; published 6 February 2023)

We propose a scheme to dissipatively produce steady-state entanglement in a two-qubit system, via an interaction with a bosonic mode. The system is driven into a stationary entangled state, while we compensate the mode dissipation by injecting energy via a coherent pump field. We also present a scheme which allows us to adiabatically transfer all the population to the desired entangled state. The dynamics leading to the entangled state in these schemes can be understood in analogy with electromagnetically induced transparency and stimulated Raman adiabatic passage, respectively.

DOI: [10.1103/PhysRevA.107.023706](https://doi.org/10.1103/PhysRevA.107.023706)

I. INTRODUCTION

Entanglement is the clearest nonclassical signature of quantum physics. A composite system is considered to be entangled when the quantum state that describes it is inseparable; i.e., it is impossible to write it as a product of the states of each subsystem [1]. In the past decades, entangled states have been the subject of great interest, presenting themselves as a resource for several quantum schemes and applications such as quantum communication [2–4], quantum computation [5], metrology [6], and quantum sensing [7].

The success of the aforementioned applications and tests often depends on the ability to generate long-lived entangled states. However, in a realistic situation, the system will interact with the environment. This will inevitably lead to the deterioration of the entangled state, which is sensitive to decoherence [1]. For this reason, entanglement preservation schemes have gained great prominence. Among the proposed methods to minimize unwanted decoherence, we should mention the use of decoherence-free subspaces [8,9], quantum error correction codes [10,11], weak measurements [12,13], and the quantum Zeno effect [14,15].

Instead of aiming to prevent decoherence, a different strategy involves engineering the system-environment interaction to *generate* entangled states; these are called dissipation-assisted entanglement generation methods [16–18]. Since this idea was presented, numerous implementations have been proposed and experimentally realized using several physical platforms, such as cavity QED [19–25], superconducting qubits [26–29], macroscopic atomic ensembles [30,31],

Rydberg atoms [32–34], quantum dots [35,36], and trapped ions [37–42]. Another widely studied approach is the creation of long-lived entangled states via stimulated Raman adiabatic passage (STIRAP), fractional STIRAP, and rapid adiabatic passage [43–48], since it offers robustness against decoherence by not populating lossy states.

In this paper we propose two schemes for producing highly entangled states in a system of two nondegenerate qubits. It is known that, in some systems, it is possible to manipulate the degree of entanglement between two qubits via Stark shifts of their electronic levels [21,49,50]. Here, however, we show that the symmetry in the energy shifts between the emitters with respect to the bosonic mode actually allows us to achieve a stronger entanglement. By considering their effective interaction through a bosonic mode, such as an optical cavity or a motional mode, we are able to achieve a stronger coupling between the qubits without needing to place the qubits particularly close together. This interaction with the quantized mode provides a coupling regime strong enough so that the timescales of the effective interactions are much faster than the qubit relaxation, leading to higher degrees of entanglement. This shows that the distinguishability between the quantum emitters can be an advantage in the quest for the producing highly entangled states. We are able to achieve a maximally entangled steady state, which is maintained by injecting power via a pump field.

We show that the dynamics leading to the highly entangled two-qubit state can be understood by comparison with the electromagnetically induced transparency (EIT) regime [51]. In that same analogy, but restricting ourselves to the subspace of just a single excitation, we are able to drive the system into an entangled state via a STIRAP-like process.

II. MODEL

Let us consider a system of two qubits, with different resonance frequencies $\omega_e^{(1)}$ and $\omega_e^{(2)}$, which are coupled to

*murilo.oliveira@df.ufscar.br

†Present address: Institute for Quantum Optics and Quantum Information, Austrian Academy of Sciences, Vienna, Austria.

‡Present address: Division of Physics, Mathematics, and Astronomy, California Institute of Technology, Pasadena, CA 91125, USA.

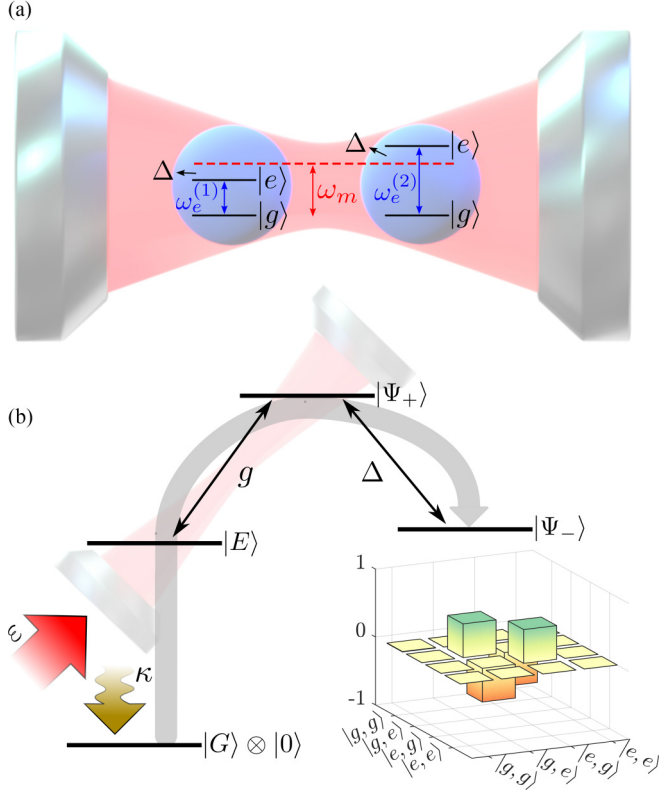


FIG. 1. (a) Two nondegenerate qubits, with both ground states coupled to the bosonic mode of frequency ω_m , detuned by $\pm\Delta$. (b) Level scheme of the same system, but now in the basis up to one excitation: $|G\rangle \otimes |0\rangle$, $|E\rangle = |G\rangle \otimes |1\rangle$, and $|\Psi_{\pm}\rangle = |\Phi_{\pm}\rangle \otimes |0\rangle$, where $|G\rangle = |g, g\rangle$ and $|\Phi_{\pm}\rangle = (|e, g\rangle \pm |g, e\rangle)/\sqrt{2}$. Here, g promotes transitions from $|E\rangle$ to $|\Psi_{+}\rangle$, while Δ promotes transitions from $|\Psi_{+}\rangle$ to $|\Psi_{-}\rangle$. We consider a pump field, of strength ε , continuously injecting energy into the mode to combat decay from the mode with rate κ . The inset in panel (b) shows the entangled steady-state partial density matrix, where the bosonic mode has been traced out.

the same bosonic mode with frequency ω_m , as illustrated in Fig. 1(a). Here, the bosonic mode is symmetrically detuned from each of the qubits, so that $\omega_e^{(1)} = \omega_m - \Delta$ and $\omega_e^{(2)} = \omega_m + \Delta$. In the Schrödinger picture, the system Hamiltonian reads as follows ($\hbar = 1$):

$$\hat{H} = \omega_e^{(1)}\hat{\sigma}_{ee}^{(1)} + \omega_e^{(2)}\hat{\sigma}_{ee}^{(2)} + \omega_m\hat{a}^{\dagger}\hat{a} + g[\hat{a}(\hat{\sigma}_{+}^{(1)} + \hat{\sigma}_{+}^{(2)}) + \text{H.c.}], \quad (1)$$

where $\hat{\sigma}_{+}^{(k)} = |e\rangle\langle g|$, $\hat{\sigma}_{-}^{(k)} = |g\rangle\langle e|$, and $\hat{\sigma}_{ee}^{(k)} = |e\rangle\langle e|$ are the raising, lowering, and excited-state population operators, respectively, acting on the k th qubit (with $k \in \{1, 2\}$). Without loss of generality, we define the ground-state energy to be zero. \hat{a} (\hat{a}^{\dagger}) is the annihilation (creation) operator of the bosonic mode, g is the coupling strength between the bosonic mode and each of the qubits, and H.c. stands for the Hermitian conjugate.

For convenience, we move to the interaction picture, make the rotating-wave approximation, and move to a rotating referential of relative coordinates in which both qubits are stationary, thus eliminating the Hamiltonian time dependence.

Then, Eq. (1) becomes

$$\hat{\mathcal{H}} = \Delta(\hat{\sigma}_{ee}^{(1)} - \hat{\sigma}_{ee}^{(2)}) + g[\hat{a}(\hat{\sigma}_{+}^{(1)} + \hat{\sigma}_{+}^{(2)}) + \text{H.c.}], \quad (2)$$

To account for decoherence, we consider our system to be in a weak system-environment coupling regime, which allows us to use the Lindblad master equation [52] at temperature $T = 0$ K. The assumption of zero temperature is reasonable since we work within the optical regime, where the number of thermal photons remains negligible even for room temperatures. Thus, we obtain the dynamical equations for the density matrix ρ :

$$\dot{\rho} = -i[\hat{\mathcal{H}}, \rho] + \mathcal{L}_q^{(1)} + \mathcal{L}_q^{(2)} + \mathcal{L}_m, \quad (3)$$

where

$$\mathcal{L}_q^{(k)} = \Gamma(2\hat{\sigma}_{-}^{(k)}\hat{\rho}\hat{\sigma}_{+}^{(k)} - \hat{\sigma}_{ee}^{(k)}\hat{\rho} - \hat{\rho}\hat{\sigma}_{ee}^{(k)}) \quad (4)$$

is the Lindblad term that accounts for the spontaneous decay from the excited state of the k th qubit, with $k \in \{1, 2\}$ and Γ being the qubit decay rate, here assumed to be the same for both qubits. The Lindblad term

$$\mathcal{L}_m = \kappa(2\hat{a}\hat{\rho}\hat{a}^{\dagger} - \hat{a}^{\dagger}\hat{a}\hat{\rho} - \hat{\rho}\hat{a}^{\dagger}\hat{a}) \quad (5)$$

accounts for decay of the bosonic mode, where κ is the decay rate.

III. STEADY-STATE ENTANGLEMENT PRODUCTION

To describe the main mechanism responsible for the generation of entanglement, we restrict ourselves, for the moment, to the single-excitation subspace, which is composed of the following three states: $|E\rangle = |G\rangle \otimes |1\rangle$ and $|\Psi_{\pm}\rangle = |\Phi_{\pm}\rangle \otimes |0\rangle$, where $|G\rangle = |g, g\rangle$ and $|\Phi_{\pm}\rangle = (|e, g\rangle \pm |g, e\rangle)/\sqrt{2}$. $|\Phi_{\pm}\rangle$ are maximally entangled two-qubit states. In this subspace, the reduced Hamiltonian is

$$\hat{\mathcal{H}} = \Delta|\Psi_{-}\rangle\langle\Psi_{+}| + \sqrt{2}g|\Psi_{+}\rangle\langle E| + \text{H.c.} \quad (6)$$

In analogy with the typical three-level Λ systems, we consider that $|E\rangle$ and $|\Psi_{-}\rangle$ play the roles of the two ground states, while $|\Psi_{+}\rangle$ is the excited state, as depicted in Fig. 1(b). According to Eq. (6), the transitions $|E\rangle \leftrightarrow |\Psi_{+}\rangle$ and $|\Psi_{-}\rangle \leftrightarrow |\Psi_{+}\rangle$ have effective coupling strengths $\sqrt{2}g$ and Δ , respectively. The Hamiltonian in Eq. (6) has a *dark eigenstate* (an eigenstate without a $|\Psi_{+}\rangle$ component) given by

$$|D\rangle = -\frac{\Delta}{\sqrt{\Delta^2 + 2g^2}}|E\rangle + \frac{\sqrt{2}g}{\sqrt{\Delta^2 + 2g^2}}|\Psi_{-}\rangle. \quad (7)$$

Just as in other three-level systems [51], when the condition $g \gg \Delta$ is fulfilled, the dark state $|D\rangle$ transforms to $|\Psi_{-}\rangle$, which is our maximally entangled target state.

A significant difference between our system and a typical three-level Λ system is the fact that neither $|E\rangle$ nor $|\Psi_{-}\rangle$ is actually a ground state. Because of this, the system keeps spontaneously decaying to the true zero-energy ground state $|G\rangle \otimes |0\rangle$. For this reason, the analogy becomes more accurate as the mode dissipation rate κ and the spontaneous decay rate Γ become negligible ($\kappa, \Gamma \ll g, \Delta$). Then the system effectively remains in the one-excitation subspace. One way to circumvent the decay and maintain the system in the one-excitation subspace is to keep injecting energy into the mode.

We consider this energy injection as an additional term,

$$\hat{H}_{\text{pump}} = \varepsilon(\hat{a}^\dagger + \hat{a}), \quad (8)$$

of the system's Hamiltonian, where ε is the pump strength.

To characterize the steady-state entanglement between the qubits, we choose the monotone quantifier concurrence [53,54]. We numerically simulate the full system dynamics, taking into account the decoherence and also higher excited states. To this end, we consider a sufficiently large Fock space dimension that depends on the adopted pump field strength ε and consequently on the respective expected mean number of excitations in the system. The concurrence is derived from the steady-state density matrix, which we obtain using the Quantum Toolbox in PYTHON (QUTIP) [55], after the mode is traced out.

As shown in Fig. 2(a), we obtain a strong entanglement within a large region of parameters Δ and g for $\varepsilon = \kappa$. Moreover, we see that satisfying the EIT condition $g \gg \Delta$ is a necessary but not sufficient condition to reach our maximally entangled target state. We have chosen four sets of parameters to illustrate the system dynamics: set A shows the situation where $g \ll \Delta$ and the population is led to the respective dark state, which has a $|G\rangle$ character [see Eq. (7)], and no entanglement is observed. In set B, we have $g = \Delta$ which leads to a weakly entangled dark state given by a mixture of $|G\rangle$ and $|\Phi_{-}\rangle$. In set C, we have an interesting situation where the EIT condition $g \gg \Delta$ is fulfilled and the dark state assumes a $|\Phi_{-}\rangle$ character, but the detuning is so small that it takes too long to populate $|\Phi_{-}\rangle$, and since the system keeps decaying to the true ground state $|G\rangle \otimes |0\rangle$, the entanglement is affected. Set D shows a near-optimal situation, with $g \gg \Delta$ and $\Delta \gg \Gamma$, driving approximately all the population to the dark state $|\Phi_{-}\rangle$.

In a similar way, Fig. 2(b) shows a map of concurrence in the steady state as a function of g and ε , with the constraint $\Delta = 0.1g$. This ratio between g and Δ was chosen to obtain maximum concurrence based on the results shown in Fig. 2(a). In Fig. 2(b), we notice a parameter region with a maximum plateau of concurrence as a function of ε for $g > \kappa$. The value $\varepsilon = \kappa$ is close to the point where it is possible to obtain a high degree of entanglement even for weak coupling strengths ($g \lesssim \kappa$).

In Fig. 2(c) we show the behavior of the concurrence as a function of the detuning for a fixed value of $g = \kappa$. We observe that the concurrence decreases significantly when we move away from the optimal point $\Delta \approx 0.1g$. This finding is in accordance with what was previously discussed for the parameters sets A and C. This optimal ratio between g and Δ is influenced by the system's decay rate Γ . A reduced value of Γ allows us to achieve entanglement for smaller detunings. For $\Gamma = 0$, even an infinitesimal detuning would eventually take the system to $|\Phi_{-}\rangle$. Figure 2(c) shows that the spontaneous decay reduces the entanglement even for the optimal case D; the concurrence decreases exponentially for $\Gamma > 5 \times 10^{-4}\kappa$.

Focusing on the entanglement dynamics, we show in Fig. 2(d) the concurrence over time for the cases A, B, C, and D, where we observe different timescales to achieve the maximum entanglement for each curve, respectively. We also include a visual representation of the time-evolved partial density matrix, where the bosonic mode has been traced out,

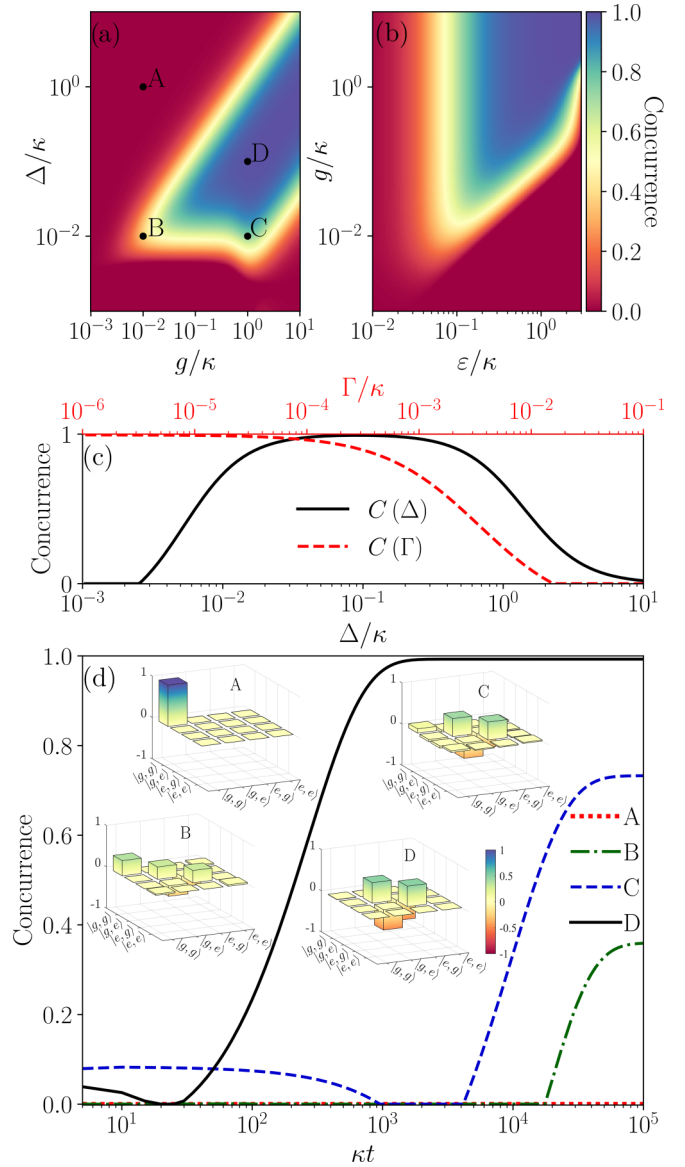


FIG. 2. Entanglement generation using the steady-state method. (a) Colormap showing the concurrence of the steady state as a function of Δ/κ and g/κ . Points A to D are referred to in panel (d). (b) Colormap showing the concurrence of the steady state as a function of g and ε (with Δ given by the constraint $\Delta = 0.1g$). (c) Concurrence as a function of the spontaneous decay rate Γ of each of the two qubits (top x axis) and as a function of the detuning (bottom x axis). (d) Concurrence as a function of time for different parameter sets, given in panel (a). The concurrence generally grows and then stabilizes. The insets in panel (d) show the steady-state partial density matrix of each curve, where the mode has been traced out. For all panels except panel (b), the pump strength was set to $\varepsilon = \kappa$. The spontaneous decay rate of each qubit was fixed at $\Gamma = 10^{-5}\kappa$, except for the red dashed curve in panel (c). The constant parameters in panel (c) are given by point D in panel (a).

showing that we achieve the maximally entangled target state $|\Phi_{-}\rangle$ for the near-optimal set of parameters D.

So far, we have adopted a generic description of the system, since our scheme proves to be quite versatile in terms of how many experimental platforms on which it could be imple-

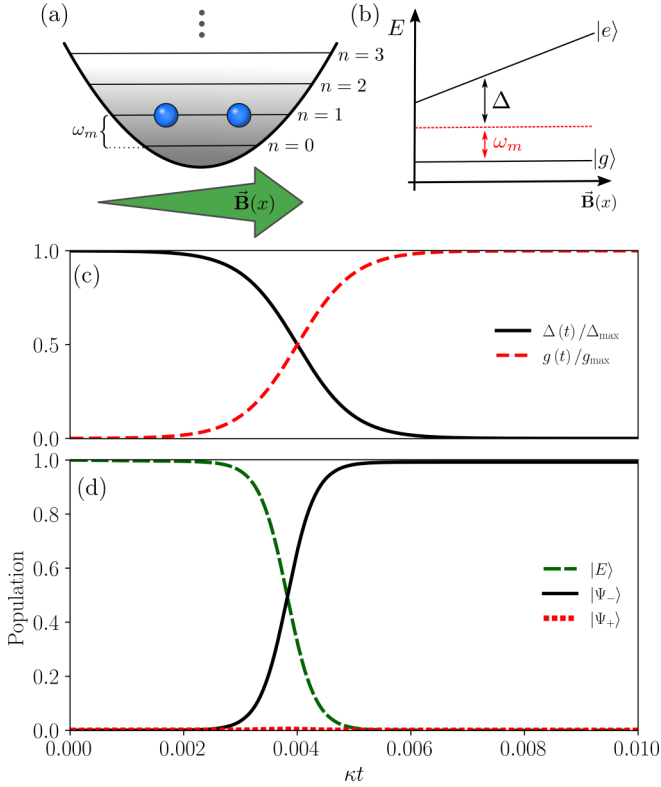


FIG. 3. Entanglement generation—adiabatic method with tunable g and Δ . (a) Two two-level ions are trapped in a harmonic potential and coupled to the same phonon mode. The ions are subjected to a magnetic field gradient, which promotes different energy shifts to their excited states, recovering the system illustrated in Fig. 1(a). (b) Pictorial representation of the energy shifts in the ions' excited states due to a magnetic field gradient, as a function of their position in the trap. (c) Time evolution of the parameters $g(t)$ and $\Delta(t)$ as described in Eqs. (9) and (10), with the corresponding population changes in panel (d). We considered for all simulations the following adopted parameters: $\Gamma = 10^{-3}\kappa$, $g_{\max} = \Delta_{\max} = 2 \times 10^4\kappa$, $t_0 = 4 \times 10^{-3}\kappa$, and $\lambda = 10^3\kappa$.

mented: optical cavities with neutral atoms coupled to the same cavity mode [56,57], superconducting artificial atoms coupled to waveguides [58,59], and ions trapped in the same harmonic potential, coupled via laser with Jaynes-Cummings type interaction and interaction with a collective vibrational mode [60].

IV. ADIABATIC PROCESS

Inspired by the schemes to counteract decoherence developed for multilevel atoms, we propose a STIRAP-like process to efficiently populate the entangled state $|\Psi_{-}\rangle$. For the sake of clarity and simplicity, during this section we restrict ourselves to the physical system of trapped ions.

To this end, let us consider the case of two ions confined in a harmonic potential, as depicted in Fig. 3(a). In addition, let us also consider that two electronic levels of the ions are driven by a monochromatic laser close to resonance. The ions are subjected to a magnetic field gradient, thus allowing them to experience different energy shifts of their excited states,

resembling the system illustrated in Fig. 1(a). The bosonic mode is formed by the external degrees of freedom of the ions. For simplicity, we only consider the collective center-of-mass motional mode described by a harmonic oscillator of frequency ω_m . Absorption and stimulated emission of photons due to the interaction with the laser leads to electronic transitions, but due to the momentum of the absorbed and emitted photons may also change the ions' motional state, thus coupling the internal electronic dynamics and the external phonon dynamics of the ions [61–63]. In the Lamb-Dicke regime, the laser can be tuned in frequency to be either directly in resonance to the atomic transition, where the motional state is preserved, or in resonance to a blue or red sideband, where a phonon is generated or annihilated upon absorption of a laser photon. When tuned to the red motional sideband resonance, we recover a Hamiltonian in the form of Eq. (2).

To perform the adiabatic population transfer between the two dark states of the one-excitation subspace [see Eq. (7)], the system must be initially prepared in the state $|E\rangle$, which consists of the two ions in the ground state and the motional state with one excitation; the latter can be prepared by exciting one of the ions and then by letting it exchange energy with the vibration mode via a red sideband interaction. The initial state $|E\rangle$ corresponds to the dark state when $\Delta \gg g$. By reversing this condition to $g \gg \Delta$, the dark state adiabatically transforms to $|\Psi_{-}\rangle$. In the proposed implementation, we can manipulate both the coupling strength g and the detuning Δ by changing the power of a laser resonant to the red sideband transition and by varying the magnetic field gradient, respectively. To illustrate, we here consider the time variation of g and Δ as

$$g(t) = \frac{g_{\max}}{2} [1 + \tanh \lambda(t - t_0)], \quad (9)$$

$$\Delta(t) = \frac{\Delta_{\max}}{2} [1 - \tanh \lambda(t - t_0)], \quad (10)$$

where g_{\max} and Δ_{\max} are respectively the maximum values of the coupling constant and the detuning. The parameter t_0 is the time at which this function reaches its respective half-maximum value $\Delta_{\max}/2$. The adiabaticity of the process is controlled by λ , which determines the timescale of the parameter swap and, consequently, how fast the parameters are changed. The specific choice of function is not crucial to the method, as long as it guarantees a near-adiabatic inversion of parameters. The parameter swap previously described by Eqs. (9) and (10) is shown in Fig. 3(c).

In Fig. 3(d), we can see how the populations in the three states of the single-excitation subspace evolve through time, showing that we coherently transfer the population from $|E\rangle$ to $|\Psi_{-}\rangle$ ($\langle \Psi_{-} | \Psi_{-} \rangle > 0.99$) before the mode dissipation starts to be relevant.

This scheme can also be applied to other experimental platforms. However, these might not allow a perfect control over both parameters at the same time, e.g., a fixed g and a tunable Δ as observed in systems where the coupling constant sometimes is an intrinsic value, such as in superconducting circuits. It is important to mention that the parameter swap we are proposing, although very similar to the ones observed in Raman chirped adiabatic passages, does not involve any changes in the field frequencies during the process. With that

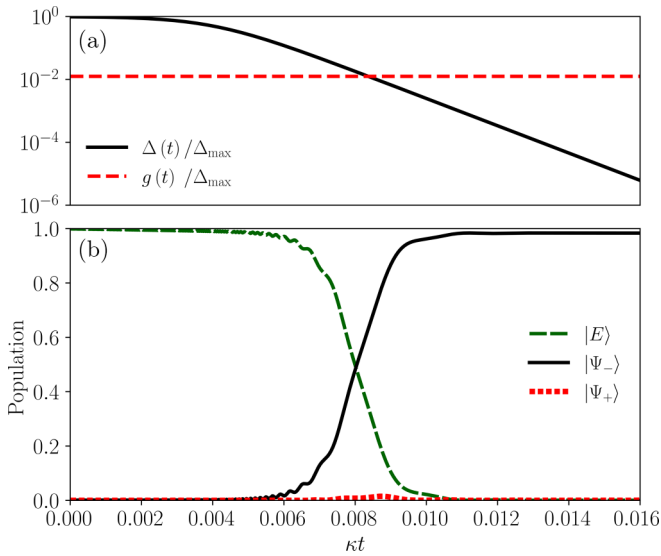


FIG. 4. Entanglement generation—adiabatic method. (a) Time evolution of g and Δ , with Δ varying accordingly to Eq. (10) and a constant g . (b) Population changes over time. We considered $\Gamma = 10^{-3}\kappa$, $\Delta_{\max} = 2 \times 10^5\kappa$, $g = 2.5 \times 10^3\kappa$, $t_0 = 4 \times 10^{-3}/\kappa$, and $\lambda = 5 \times 10^2\kappa$.

being said, in order to show that even in this situation we can achieve a high degree of entanglement, we assume g to be constant and we vary Δ in time, according to Eq. (10), as shown in Fig. 4(a). Setting the value of g that ensures the initial and final conditions $\Delta \gg g$ and $g \gg \Delta$, respectively, we make the parameter swapping as smooth as possible. On the other hand, the lack of control over g restricts the timescale of the population transfer to maintain the adiabaticity during the parameter swap. Nevertheless, one can still perform a STIRAP-like process, obtaining a highly entangled final state, as shown in Fig. 4(b), with a negligible population of the state $|\Psi_{+}\rangle$.

V. CONCLUSION

In conclusion, here we present two strategies for producing maximally entangled states in a system of two nondegenerate qubits coupled to a single bosonic mode. In both cases, we use

a direct analogy with ordinary three-level atomic systems in the Λ configuration and the EIT phenomenon, which allows us to draw a parallel with the processes of optical pumping and adiabatic population transfer.

In the first proposed scheme, we show that it is possible to generate steady-state entanglement with concurrence $C > 0.99$. Moreover, we show that the symmetry between the qubits with respect to the bosonic mode is beneficial for the generation of entanglement. As for the second scheme, we generate a highly entangled state by means of an adiabatic process, and we achieve a population over 99% in the state $|\Psi_{-}\rangle$. We emphasize that this was done even considering nonideal situations, where there is no complete control over g and Δ . In ideal cases, where both parameters can be controlled simultaneously, the adiabatic process can be controlled more efficiently, which leads to a perfectly coherent transfer of populations.

The results presented in this work, besides indicating alternative ways to generate highly entangled states in a simple way, have potential application in several experimental platforms, such as trapped ions and quantum dot molecules coupled to a cavity mode.

ACKNOWLEDGMENTS

C.J.V.-B., R.B., and M.H.O. thank the the National Council for Scientific and Technological Development (CNPq) for support through Grants No. 311612/2021-0, 141247/2018-5, No. 409946/2018-4, and No. 313886/2020-2, and they thank the São Paulo Research Foundation (FAPESP) for support through Grants No. 2020/00725-9, No. 2019/13143-0, No. 2019/11999-5, and No. 2018/15554-5. R.B. acknowledges support by the French government through the UCA-JEDI Investments in the Future project managed by the National Research Agency, project ANR-15-IDEX-01. The authors also thank the Joint Brazilian-Swedish Research Collaboration (CAPES-STINT) for support under Grants No. 88887.304806/2018-00 and No. BR2018-8054. M.H., G.H., C.Z. are grateful for the support by the Knut and Alice Wallenberg Foundation (through the Wallenberg Centre for Quantum Technology [WACQT]), by Olle Enkvists Stiftelse (Project No 204-0283), by Carl Trygger Stiftelse (Grant No. CTS 19-139), and by the Swedish Research Council (Trapped Rydberg Ion Quantum Simulator).

-
- [1] R. Horodecki, P. Horodecki, M. Horodecki, and K. Horodecki, Quantum entanglement, *Rev. Mod. Phys.* **81**, 865 (2009).
 - [2] A. K. Ekert, Quantum Cryptography Based on Bell's Theorem, *Phys. Rev. Lett.* **67**, 661 (1991).
 - [3] C. H. Bennett, G. Brassard, C. Crépeau, R. Jozsa, A. Peres, and W. K. Wootters, Teleporting an Unknown Quantum State via Dual Classical and Einstein-Podolsky-Rosen Channels, *Phys. Rev. Lett.* **70**, 1895 (1993).
 - [4] C. H. Bennett and D. P. DiVincenzo, Quantum information and computation, *Nature (London)* **404**, 247 (2000).
 - [5] D. Gottesman and I. L. Chuang, Demonstrating the viability of universal quantum computation using teleportation and single-qubit operations, *Nature (London)* **402**, 390 (1999).
 - [6] V. Giovannetti, S. Lloyd, and L. Maccone, Quantum Metrology, *Phys. Rev. Lett.* **96**, 010401 (2006).
 - [7] C. L. Degen, F. Reinhard, and P. Cappellaro, Quantum sensing, *Rev. Mod. Phys.* **89**, 035002 (2017).
 - [8] D. A. Lidar, I. L. Chuang, and K. B. Whaley, Decoherence-Free Subspaces for Quantum Computation, *Phys. Rev. Lett.* **81**, 2594 (1998).
 - [9] L. Viola and S. Lloyd, Dynamical suppression of decoherence in two-state quantum systems, *Phys. Rev. A* **58**, 2733 (1998).
 - [10] A. M. Steane, Error Correcting Codes in Quantum Theory, *Phys. Rev. Lett.* **77**, 793 (1996).
 - [11] E. Knill and R. Laflamme, Theory of quantum error-correcting codes, *Phys. Rev. A* **55**, 900 (1997).

- [12] Q. Sun, M. Al-Amri, L. Davidovich, and M. S. Zubairy, Reversing entanglement change by a weak measurement, *Phys. Rev. A* **82**, 052323 (2010).
- [13] Y.-S. Kim, J.-C. Lee, O. Kwon, and Y.-H. Kim, Protecting entanglement from decoherence using weak measurement and quantum measurement reversal, *Nat. Phys.* **8**, 117 (2012).
- [14] P. Facchi, D. A. Lidar, and S. Pascazio, Unification of dynamical decoupling and the quantum Zeno effect, *Phys. Rev. A* **69**, 032314 (2004).
- [15] S. Maniscalco, F. Francica, R. L. Zaffino, N. L. Gullo, and F. Plastina, Protecting Entanglement via the Quantum Zeno Effect, *Phys. Rev. Lett.* **100**, 090503 (2008).
- [16] S. Diehl, A. Micheli, A. Kantian, B. Kraus, H. P. Büchler, and P. Zoller, Quantum states and phases in driven open quantum systems with cold atoms, *Nat. Phys.* **4**, 878 (2008).
- [17] B. Kraus, H. P. Büchler, S. Diehl, A. Kantian, A. Micheli, and P. Zoller, Preparation of entangled states by quantum Markov processes, *Phys. Rev. A* **78**, 042307 (2008).
- [18] F. Verstraete, M. M. Wolf, and J. Ignacio Cirac, Quantum computation and quantum-state engineering driven by dissipation, *Nat. Phys.* **5**, 633 (2009).
- [19] M. B. Plenio, S. F. Huelga, A. Beige, and P. L. Knight, Cavity-loss-induced generation of entangled atoms, *Phys. Rev. A* **59**, 2468 (1999).
- [20] S. Nicolosi, A. Napoli, A. Messina, and F. Petruccione, Dissipation-induced stationary entanglement in dipole-dipole interacting atomic samples, *Phys. Rev. A* **70**, 022511 (2004).
- [21] X. Wang and S. G. Schirmer, Generating maximal entanglement between non-interacting atoms by collective decay and symmetry breaking, [arXiv:1005.2114](https://arxiv.org/abs/1005.2114).
- [22] M. J. Kastoryano, F. Reiter, and A. Søndberg Sørensen, Dissipative Preparation of Entanglement in Optical Cavities, *Phys. Rev. Lett.* **106**, 090502 (2011).
- [23] E. del Valle, Steady-state entanglement of two coupled qubits, *J. Opt. Soc. Am. B* **28**, 228 (2011).
- [24] B. Casabone, K. Friebe, B. Brandstätter, K. Schüppert, R. Blatt, and T. E. Northup, Enhanced Quantum Interface with Collective Ion-Cavity Coupling, *Phys. Rev. Lett.* **114**, 023602 (2015).
- [25] P. Samutpraphoot, P. L. Ocola, H. Bernien, C. Senko, V. Vuletić, and M. D. Lukin, Strong Coupling of Two Individually Controlled Atoms via a Nanophotonic Cavity, *Phys. Rev. Lett.* **124**, 063602 (2020).
- [26] S. Shankar, M. Hatridge, Z. Leghtas, K. M. Sliwa, A. Narla, U. Vool, S. M. Girvin, L. Frunzio, M. Mirrahimi, and M. H. Devoret, Autonomously stabilized entanglement between two superconducting quantum bits, *Nature (London)* **504**, 419 (2013).
- [27] M. E. Kimchi-Schwartz, L. Martin, E. Flurin, C. Aron, M. Kulkarni, H. E. Tureci, and I. Siddiqi, Stabilizing Entanglement via Symmetry-Selective Bath Engineering in Superconducting Qubits, *Phys. Rev. Lett.* **116**, 240503 (2016).
- [28] Y. Liu, S. Shankar, N. Ofek, M. Hatridge, A. Narla, K. M. Sliwa, L. Frunzio, R. J. Schoelkopf, and M. H. Devoret, Comparing and Combining Measurement-Based and Driven-Dissipative Entanglement Stabilization, *Phys. Rev. X* **6**, 011022 (2016).
- [29] E. Doucet, F. Reiter, L. Ranzani, and A. Kamal, High fidelity dissipation engineering using parametric interactions, *Phys. Rev. Res.* **2**, 023370 (2020).
- [30] H. Krauter, C. A. Muschik, K. Jensen, W. Wasilewski, J. M. Petersen, J. I. Cirac, and E. S. Polzik, Entanglement Generated by Dissipation and Steady State Entanglement of Two Macroscopic Objects, *Phys. Rev. Lett.* **107**, 080503 (2011).
- [31] A. C. Santos, A. Cidrim, C. J. Villas-Boas, R. Kaiser, and R. Bachelard, Generating long-lived entangled states with free-space collective spontaneous emission, *Phys. Rev. A* **105**, 053715 (2022).
- [32] D. D. Bhaktavatsala Rao and K. Mølmer, Dark Entangled Steady States of Interacting Rydberg Atoms, *Phys. Rev. Lett.* **111**, 033606 (2013).
- [33] A. W. Carr and M. Saffman, Preparation of Entangled and Antiferromagnetic States by Dissipative Rydberg Pumping, *Phys. Rev. Lett.* **111**, 033607 (2013).
- [34] X. Q. Shao, J. H. Wu, X. X. Yi, and G.-L. Long, Dissipative preparation of steady Greenberger-Horne-Zeilinger states for Rydberg atoms with quantum zeno dynamics, *Phys. Rev. A* **96**, 062315 (2017).
- [35] M. A. Antón, Phonon-assisted entanglement between two quantum dots coupled to a plasmonic nanocavity, *Opt. Commun.* **508**, 127811 (2022).
- [36] A. Hichri, S. Jaziri, and R. Ferreira, Entangled Bell states of two electrons in coupled quantum dots—Phonon decoherence, *Phys. E* **24**, 234 (2004).
- [37] J. T. Barreiro, M. Müller, P. Schindler, D. Nigg, T. Monz, M. Chwalla, M. Hennrich, C. F. Roos, P. Zoller, and R. Blatt, An open-system quantum simulator with trapped ions, *Nature (London)* **470**, 486 (2011).
- [38] Y. Lin, J. P. Gaebler, F. Reiter, T. R. Tan, R. Bowler, A. S. Sørensen, D. Leibfried, and D. J. Wineland, Dissipative production of a maximally entangled steady state of two quantum bits, *Nature (London)* **504**, 415 (2013).
- [39] C. D. B. Bentley, A. R. R. Carvalho, D. Kielpinski, and J. J. Hope, Detection-Enhanced Steady State Entanglement with Ions, *Phys. Rev. Lett.* **113**, 040501 (2014).
- [40] K. P. Horn, F. Reiter, Y. Lin, D. Leibfried, and C. P. Koch, Quantum optimal control of the dissipative production of a maximally entangled state, *New J. Phys.* **20**, 123010 (2018).
- [41] D. C. Cole, J. J. Wu, S. D. Erickson, P.-Y. Hou, A. C. Wilson, D. Leibfried, and F. Reiter, Dissipative preparation of W states in trapped ion systems, *New J. Phys.* **23**, 073001 (2021).
- [42] D. C. Cole, S. D. Erickson, G. Zarantonello, K. P. Horn, P.-Y. Hou, J. J. Wu, D. H. Slichter, F. Reiter, C. P. Koch, and D. Leibfried, Resource-Efficient Dissipative Entanglement of Two Trapped-Ion Qubits, *Phys. Rev. Lett.* **128**, 080502 (2022).
- [43] C. Creatore, R. T. Brierley, R. T. Phillips, P. B. Littlewood, and P. R. Eastham, Creation of entangled states in coupled quantum dots via adiabatic rapid passage, *Phys. Rev. B* **86**, 155442 (2012).
- [44] L. Chakhmakhchyan, C. Leroy, N. Ananikian, and S. Guérin, Generation of entanglement in systems of intercoupled qubits, *Phys. Rev. A* **90**, 042324 (2014).
- [45] R. G. Unanyan, B. W. Shore, and K. Bergmann, Entangled-state preparation using adiabatic population transfer, *Phys. Rev. A* **63**, 043405 (2001).
- [46] V. S. Malinovskiy and I. R. Sola, Quantum control of entanglement by phase manipulation of time-delayed pulse sequences. I, *Phys. Rev. A* **70**, 042304 (2004).
- [47] N. V. Vitanov, A. A. Rangelov, B. W. Shore, and K. Bergmann, Stimulated Raman adiabatic passage in physics, chemistry, and beyond, *Rev. Mod. Phys.* **89**, 015006 (2017).

- [48] K. Bergmann, H.-C. Nägerl, C. Panda, G. Gabrielse, E. Miloglyadov, M. Quack, G. Seyfang, G. Wichmann, S. Ospelkaus, A. Kuhn, S. Longhi, A. Szameit, P. Pirro, B. Hillebrands, X.-F. Zhu, J. Zhu, M. Drewsen, W. K. Hensinger, S. Weidt, T. Halfmann, Roadmap on STIRAP applications, *J. Phys. B: At., Mol. Opt. Phys.* **52**, 202001 (2019).
- [49] C. Hettich, C. Schmitt, J. Zitzmann, S. Kühn, I. Gerhardt, and V. Sandoghdar, Nanometer resolution and coherent optical dipole coupling of two individual molecules, *Science* **298**, 385 (2002).
- [50] J.-B. Trebbia, Q. Deplano, P. Tamarat, and B. Lounis, Tailoring the superradiant and subradiant nature of two coherently coupled quantum emitters, *Nat. Commun.* **13**, 2962 (2022).
- [51] M. Fleischhauer, A. Imamoglu, and J. P. Marangos, Electromagnetically induced transparency: Optics in coherent media, *Rev. Mod. Phys.* **77**, 633 (2005).
- [52] H.-P. Breuer and F. Petruccione, *The Theory of Open Quantum Systems* (Oxford University Press, Oxford, 2007).
- [53] S. Hill and W. K. Wootters, Entanglement of a Pair of Quantum Bits, *Phys. Rev. Lett.* **78**, 5022 (1997).
- [54] W. K. Wootters, Entanglement of Formation of an Arbitrary State of Two Qubits, *Phys. Rev. Lett.* **80**, 2245 (1998).
- [55] J. R. Johansson, P. D. Nation, and F. Nori, QuTiP 2: A Python framework for the dynamics of open quantum systems, *Comput. Phys. Commun.* **184**, 1234 (2013).
- [56] A. Neuzner, M. Körber, O. Morin, S. Ritter, and G. Rempe, Interference and dynamics of light from a distance-controlled atom pair in an optical cavity, *Nat. Photonics* **10**, 303 (2016).
- [57] S. Welte, B. Hacker, S. Daiss, S. Ritter, and G. Rempe, Photon-Mediated Quantum Gate between Two Neutral Atoms in an Optical Cavity, *Phys. Rev. X* **8**, 011018 (2018).
- [58] J. Majer, J. M. Chow, J. M. Gambetta, J. Koch, B. R. Johnson, J. A. Schreier, L. Frunzio, D. I. Schuster, A. A. Houck, A. Wallraff *et al.*, Coupling superconducting qubits via a cavity bus, *Nature (London)* **449**, 443 (2007).
- [59] J. M. Chow, A. D. Córcoles, J. M. Gambetta, C. Rigetti, B. R. Johnson, J. A. Smolin, J. R. Rozen, G. A. Keefe, M. B. Rothwell, M. B. Ketchen, and M. Steffen, Simple All-Microwave Entangling Gate for Fixed-Frequency Superconducting Qubits, *Phys. Rev. Lett.* **107**, 080502 (2011).
- [60] R. Blatt and D. Wineland, Entangled states of trapped atomic ions, *Nature (London)* **453**, 1008 (2008).
- [61] H. Häffner, C. F. Roos, and R. Blatt, Quantum computing with trapped ions, *Phys. Rep.* **469**, 155 (2008).
- [62] R. Blatt and C. F. Roos, Quantum simulations with trapped ions, *Nat. Phys.* **8**, 277 (2012).
- [63] D. Estève, J.-M. Raimond, and J. Dalibard, Quantum entanglement and information processing, *Lecture Notes of the Les Houches Summer School 2003*, Vol. 79 (Elsevier, Amsterdam, 2004).